Ceramics International 45 (2019) 20258–20265

Contents lists available at ScienceDirect

Ceramics International

journal homepage: www.elsevier.com/locate/ceramint

Sintering behavior of anorthite-based composite ceramics produced from natural phosphate and kaolin

A. Kenzour[a,b], H. Belhouchet[c,*], M. Kolli[a,d], S. Djouallah[a], D. Kherifi[c], S. Ramesh[e,f]

[a] Optics and Precision Mechanics Institute, University of Ferhat, Abbas Setif 1, 19000, Setif, Algeria
[b] Research Center in Industrial Technologics CRTIP, O. Box 64, Cheraga, 16014, Algiers, Algeria
[c] Physics Department, Faculty of Sciences, University Mohamed Boudiaf of M'sila, 28000, M'sila, Algeria
[d] Emerging Materials Research Unit, University of Ferhat, Abbas Setif 1, 19000, Setif, Algeria
[e] Center of Advanced Manufacturing and Material Processing, Department of Mechanical Engineering, Faculty of Engineering, University of Malaya, 50603, Kuala Lumpur, Malaysia
[f] Department of Mechanical Engineering, Faculty of Engineering, Universiti Teknologi Brunei, Bandar Seri Begawan, BE1410, Brunei

ARTICLE INFO

Keywords:
Natural phosphate
Kaolin
TCP
Anorthite
Anorthite-TCP composite

ABSTRACT

In the present work anorthite-TCP composite ceramics was produced for the first time by the solid-state sintering process involving the mixture of local natural materials of phosphate and kaolin. Various samples were prepared by varying the kaolin content from 47 to 57 wt%. The composite ceramics were sintered in air at various temperatures ranging from 1250 °C to 1325 °C and characterized to determine the phase present, relative density, Vickers microhardness, chemical bonding of molecules and microstructural development. In general, all the samples exhibited a hybrid structure, comprising of anorthite and β-TCP as the major phases with a concomitant minor phases such as TTCP and/or gehlinite depending on the temperature and kaolin content. In addition, increasing kaolin content and sintering temperature were found to be effective in improving the densification and hardness of the sintered body. In particular, sample containing 57 wt% kaolin exhibited excellent densification at 1300 °C and 1325 °C, achieving above 97% dense bodies and highest hardness of about 6.5 ± 0.7 GPa. Microstructural investigation revealed that a dense structure was evident for these samples due mainly to enhanced particle coalescence during the liquid phase sintering, resulting in pore elimination and grain coarsening.

1. Introduction

Anorthite ($CaAl_2Si_2O_8$) ceramics which belongs to the plagioclase feldspar group of minerals has been investigated by many researchers mainly due to its ability to be tailored to have different porosity levels ranging from 62 to 94% (the theoretical density of anorthite is about 2.75 gcm^{-3}), a range of thermal conductivity (0.018–0.27 W/mK), low dielectric constant of about 6.2 at 1 MHz, low thermal expansion coefficient of 4.5–4.9 × 10^{-6} K^{-1} and moderate flexural strength of 103 MPa [1–6]. This modification in the properties is achieved through microstructural and compositional control using different combination of starting precursors for calcium, alumina and silica, as well as controlling the sintering parameters [7–15]. In addition, several studies also focused on the production of anorthite composites that possess improved mechanical properties [16–21]. Typically, anorthite ceramic has been considered for several application including as potential biomaterial [21–23], porcelain stoneware [24,25], ceramics pigment [26], decorative tiles [27] and as refractory materials [5,12,14].

Kaolin is the main constituent used in the synthesis of anorthite. Zaiou et al. [7] prepared anorthite from mixing domestic kaolin (Algeria) with calcium oxide extracted from local calcium carbonate. The proportion of the kaolin to CaO was fixed at 80:20 and subjected to wet milling using a homemade vibratory milling system for 17 h, dried and calcined at 800 °C for 2 h prior to sintering (800–1100 °C). They obtained a relative density of 96% for samples sintered at 900 °C for 1 h. Ceylantekin [2] employed a combination of kaolin (Turkey), industrial calcite and alumina to produce anorthite ceramic. In this study, a stoichiometric mixture for anorthite of 1:1:2 ($CaO:Al_2O_3:2SiO_2$) composition were prepared. The author studied the effect of milling (ball-milling versus high energy planetary mono mill which was labeled as non-activated versus mechanically-activated samples) and sintering temperatures on the densification of the ceramic. It was revealed that the high energy planetary milling had a negative effect on the structure of kaolinite and resulted in grain coarsening. Nevertheless, the densification temperature for mechanically-activated anorthite was found to be 100 °C lower than that required for non-activated sample. In another

* Corresponding author.
E-mail address: hbelhou@yahoo.com (H. Belhouchet).

https://doi.org/10.1016/j.ceramint.2019.06.299
Received 11 June 2019; Received in revised form 28 June 2019; Accepted 29 June 2019
Available online 02 July 2019
0272-8842/

Table 1
XRF analysis (wt%) of the starting natural phosphate (P) and kaolin (K) used in the present work.

	P_2O_5	CaO	SiO_2	Al_2O_3	F	MgO	Fe_2O_3	K_2O	SO_3	Na_2O	L.O·I
P	26.64	47.75	2.81	0.75	3.76	1.74	0.43	0.19	2.83	1.29	11.84
K	–	0.18	45.52	38.75	–	0.023	0.04	0.03	–	0.088	15.37

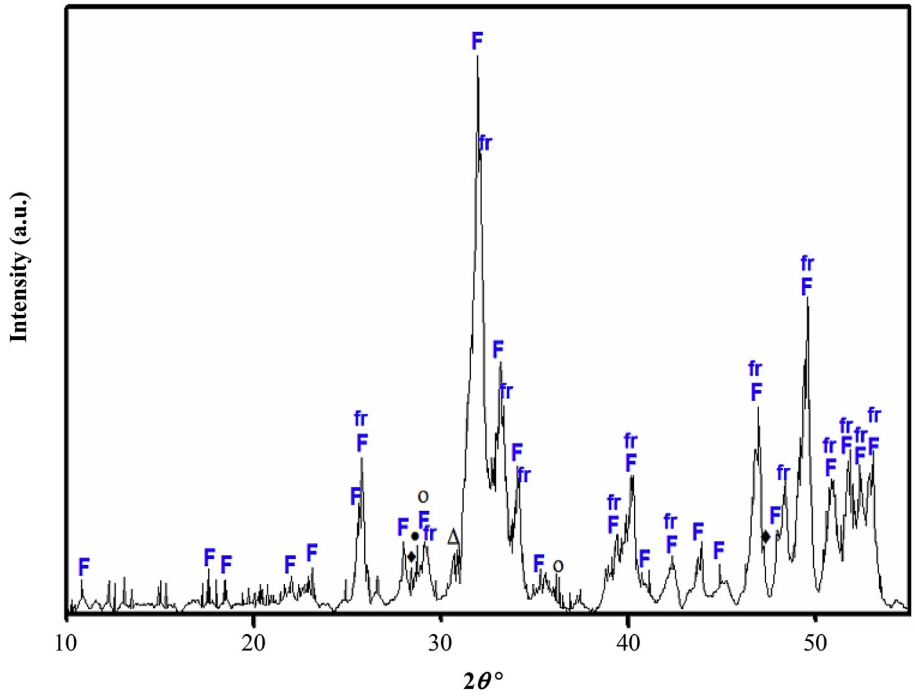

Fig. 1. XRD analysis of the starting natural phosphate powder. The phases were identified as fluorapatite (F), francolite (fr), $Ca(OH)_2$ (●), $CaCO_3$ (○), CaF_2 (♦) and dolomite (Δ).

research, Qin et al. [11] fabricated anorthite ceramic by reacting lime mud (i.e. waste obtained from an alkali recycling process in paper industry) with fly ash and sintering the mixture at various temperatures from 900 °C to 1125 °C. The authors found that samples containing 36 wt% lime mud – 64 wt% fly ash was the optimum composition and that sintering at 1100 °C was sufficient to attain a 100% anorthite phase structure. Sintering at lower temperatures resulted in the formation of secondary phases such as gehlenite, mullite and quartz. Wu et al. [12] reported the synthesis of anorthite-based composites by using municipal solid waste incinerator fly ash and kaolin by mechanical milling and sintering at 900–1300 °C. Sutcu et al. [14,15] evaluated the possibility of producing porous anorthite-based ceramic by reacting recycled paper processing residues (rich in calcium carbonate and cellulose fibers) with selective clay materials obtained from different sources and sawdust at 1100–1400 °C. The authors demonstrated the viability of producing a porous anorthite composites having a range of compressive strength (8–43 MPa) suitable for use as insulating material.

In the present study, the sintering behavior and properties of anorthite-based composite ceramics prepared by reacting natural phosphate with natural kaolin were evaluated. The primary objective was to investigate the feasibility of producing a dense ceramic composite body comprising of a hybrid phase of anorthite intermingled with tricalcium phosphate as a potential material for biomedical application.

2. Materials and methods

In the present study, natural kaolin and natural phosphate obtained from Algeria were used as the starting precursors. These minerals were used as received and the chemical composition of the powders were determined by using the X-ray fluorescence (Shimadzu Japan). Four different composite mixtures were prepared by varying the amount of kaolin (i.e. 47, 50, 54 and 57 wt %) and were subsequently labeled as P47K, P50K, P54K, P57K, respectively. This compositions were selected based on our initial study reported elsewhere [22].

In a typical powder preparation process, the starting powders were mix in distilled water and then put in a zirconia jar (250 mls volume) with zirconia balls (13 mm diameter) as the milling media. The wet milling was carried out at a rotation speed of 300 rpm for 5 h in a planetary ball mill (Fritsch P6). The resulting slurry was dried in an oven at 110 °C for 24 h and subsequently sieved through a 63 µm mesh sieve. The obtained powder was calcined at 1100 °C for 2 h at a heating rate of 8 °Cmin^{-1} to remove any residue organic compounds so as to avoid swelling or cracking of the samples during sintering.

Disc samples were uniaxial-pressed at 75 MPa and sintered under atmospheric conditions at various temperatures (i.e. 1250, 1275, 1300 and 1325 °C) for 2 h at a heating rate of 10 °C.min^{-1}.

The particle size of the calcined powders was determined using a laser scattering particle size analyzer (Horiba, LA-960). The hardness of the sintered samples was determined by using the Vickers microhardness tester at a load of 10 N applied for 10 s. The open porosity and apparent density of the sintered samples were measured by Archimedes' method using distilled water. The phases present in the powders and sintered samples were identified by XRD using Panalytical X'pert Pro3 operated at 40 kV and 40 mA, at a scan speed of 4 °min^{-1} (2θ) and step scan of 0.026°. The phase identification was accomplished by comparing the XRD signatures of the sample with that available in the International Center for Powder Diffraction Standards (ICDD) provided in the search-match program. In addition, FTIR spectra were recorded

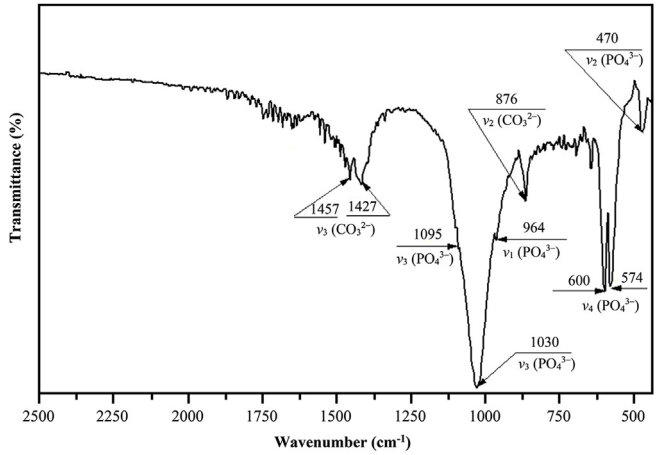

Fig. 2. FTIR spectrum of natural phosphate powder.

by using Fourier transform infrared spectroscopy (Shimadzu IRAffinity-1S) within the wave number range of 4000-400 cm^{-1}. The particle morphology and the microstructure of the fractured surface of the sintered samples was examined using FESEM (Zeiss Sigma).

3. Results and discussion

The chemical compositions of the starting materials as determined by XRF is given in Table 1. The results indicated that the natural phosphate used in this study was mainly composed of calcium oxide (CaO) and diphosphorus pentoxide (P_2O_5) as the major elements. On the other hand, the starting kaolin composed mainly of silica (SiO_2) and alumina (Al_2O_3).

The natural kaolin [22] (not shown here) composed of kaolinite as the major phase with some minor illite and quartz being observed. As for the natural phosphate, the XRD analysis (Fig. 1) shows that the powder comprised predominantly of the fluorapatite (ICDD # 015–0876) and carbonate-fluorapatite (also known as francolite, ICDD # 002–0833) as the major phases. The FTIR analysis of this material (Fig. 2) is in agreement with the XRD findings and revealed the presence of phosphate as well as carbonate groups. The FTIR spectra shows a strong band at 1030 cm^{-1} and 1095 cm^{-1} which are related to the antisymmetric vibration (stretching) mode υ_3 of (PO_4^{3-}) group [28] whereas the band at 964 cm^{-1} is associated to υ_1 (PO_4^{3-}) symmetric stretching [28]. In addition, the two strong and sharp peaks observe at 574 and at 600 cm^{-1}, beside the apparition of a peak at 470 cm^{-1}, reflect the triply degenerate antisymmetric bending υ_4 vibration and symmetric bending υ_2 vibration of (PO_4^{3-}) groups, respectively [21,22,28]. The FTIR spectra also confirmed the formation of B-type carbonate apatite as indicated by the typical CO_3^{2-} bands observed at 876, 1427 and 1457 cm^{-1} [21,28,29].

Table 2
Particle size of the calcined composite powders.

Sample	Particle size (μm)		
	D_{10}	D_{50}	D_{90}
P47K	8.30	22.78	42.91
P50K	7.19	20.28	43.14
P54K	7.80	23.07	46.57
P57K	8.96	22.92	50.38

The XRD patterns of the composite powders are shown in Fig. 3. In general, all the powders showed similar phases representing the starting precursors. The results show that the milling did not affect the phases present in the composite powders.

The particle size analysis of all the composite powders after calcination exhibited a unimodal distribution and the measured particle sizes are as given in Table 2. Similar as in the case of XRD analysis, there is not much change in the particle size measured for the composite powders.

The XRD analysis of the calcined powders at 1100 °C is shown in Fig. 4. It was found that all the mixtures revealed the formation of anorthite (ICDD # 041–1486) along with fluorapatite (ICDD # 015–0876). Moreover, some minor peaks belonging to mullite (ICDD # 002–0452) and cristobalite (ICDD # 027–0605) were detected in the mixture P57K, P54K and P50K. However, the XRD intensities of the mullite and cristobalite peaks were found to decrease with decreasing kaolin content in the samples. Also, the formation of β-TCP phase was only observed in the XRD trace of the P47K sample after calcination.

The formation of anorthite in the calcined powders can be explained from the reaction between the metakaolinite (formed by the dehydroxylation of kaolinite according to Eq. (1) at low temperatures of

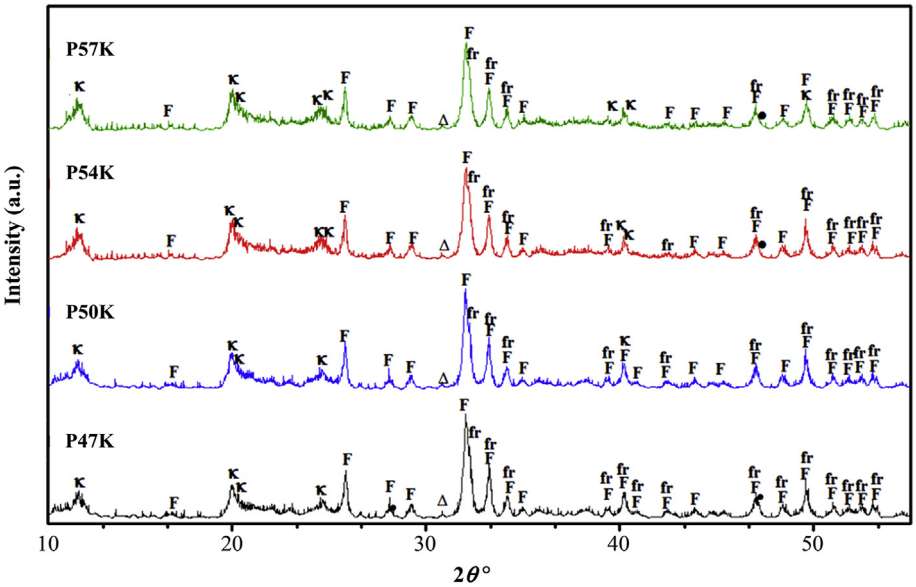

Fig. 3. XRD analysis of the as-milled composite powders before heat treatment. The phases were identified as fluorapatite (F), francolite (fr), CaF_2 (●), dolomite (Δ) and kaolinite (K).

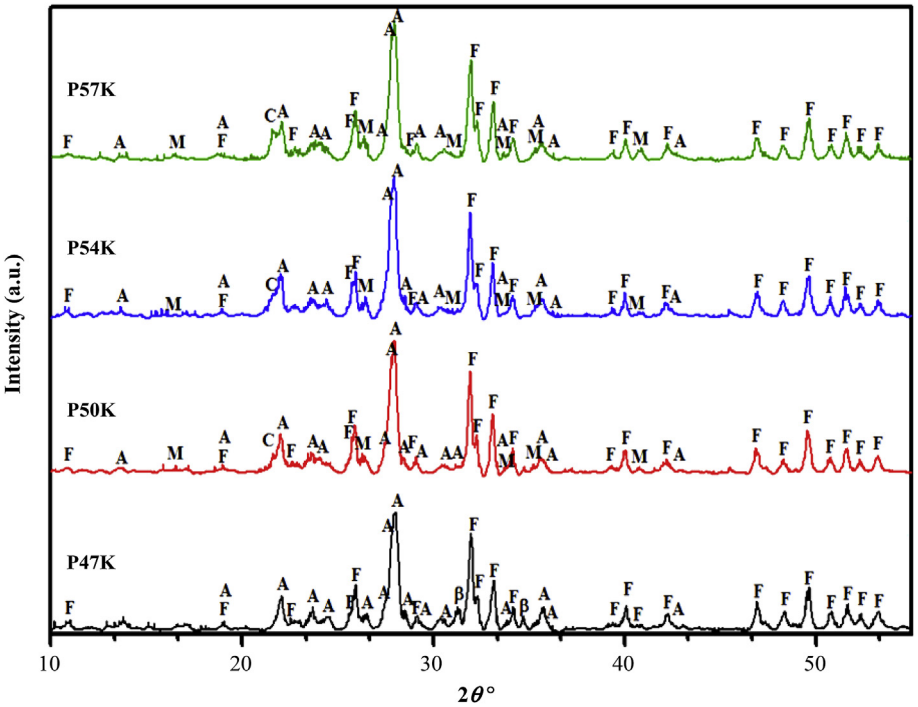

Fig. 4. XRD analysis of powder mixture calcined at 1100 °C. The phases were identified as anorthite (A), fluorapatite (F), mullite (M), cristobalite (C) and β-TCP (β).

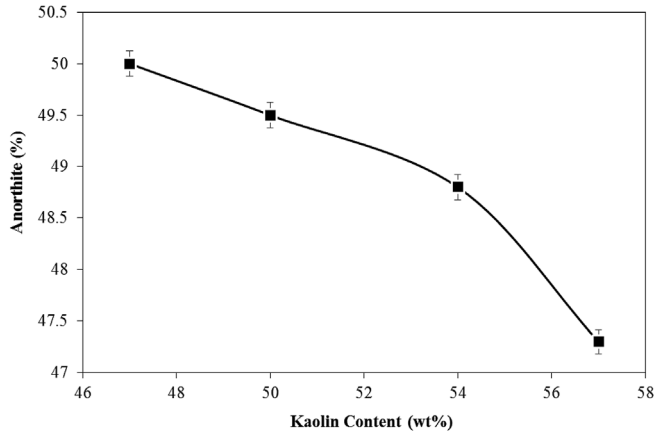

Fig. 5. Variation in the anorthite content in the sintered compacts after calcination as a function of kaolin content.

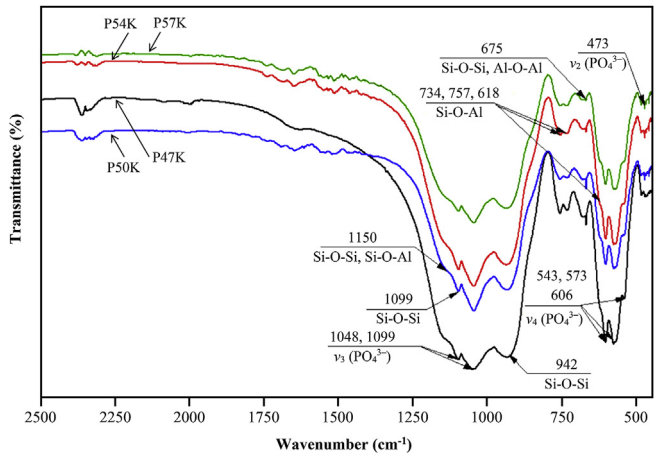

Fig. 6. FTIR spectrums of the calcined mixtures.

450–650 °C [22,30,31]) and the free CaO made available from the decomposition of calcium carbonate and dolomite present in natural phosphate based on Eq. (2) [22,31]:

$$\underset{kaolinite}{Al_2Si_2(OH)_4} \rightarrow \underset{metakaolinite}{Al_2Si_2O_7} + 2H_2O \quad (1)$$

$$\underset{metakaolinite}{Al2Si2O7} + \underset{anorthite}{CaO} \rightarrow Ca\,Al_2\,Si_2O_8 \quad (2)$$

Another possible explanation for the precipitation of anorthite could be via the decomposition of metakaolinite to form mullite and cristobalite at about 900–1000 °C [31], and the reaction of this products with the free CaO from the decomposition of calcium carbonate and dolomite according to Eq. (3) and Eq. (4), respectively.

$$\underset{metakaolinite}{3Al_2Si_2O_7} \rightarrow \underset{mullite}{3Al_2O_3.2SiO_2} + \underset{cristobalite}{4SiO_2} \quad (3)$$

$$\underset{mullite}{3Al_2O_3.2SiO_2} + \underset{cistobalite}{SiO_2} + 3CaO \rightarrow \underset{anorthite}{3Ca\,Al_2\,Si_2O_8} \quad (4)$$

The ratio of anorthite in the samples was evaluated through XRD pattern (semi-quantitative analysis) [22] and the results are plotted in Fig. 5. It can be observed that the amount of anorthite decreases with the increase of kaolin content. In addition, from the XRD patterns (Fig. 4), the peak intensities corresponding to that of mullite and cristobalite phases increased when the kaolin content increased. This is expected since the increase in kaolin content in the mixture would cause a deficit in free calcium in the mixture which hinders the development of anorthite, thus leading to the formation mullite and cristobalite phases.

The formation of anorthite has been reported by many researchers to be dependent on various processing parameters. Wu et al. [12] examined the formation of anorthite phase from mixing Chinese kaolin with different calcium sources using mechanosynthesis method for different milling times and followed by sintering at different temperatures. It was found that anorthite started to form at low temperature about 950 °C. Moreover, the crystallization of anorthite increases with the increase of sintering temperature and milling time, without the formation of any other intermediate phases. However, the authors found that the un-milled mixture showed a delay in the formation of anorthite along with the formation of an intermediate phases

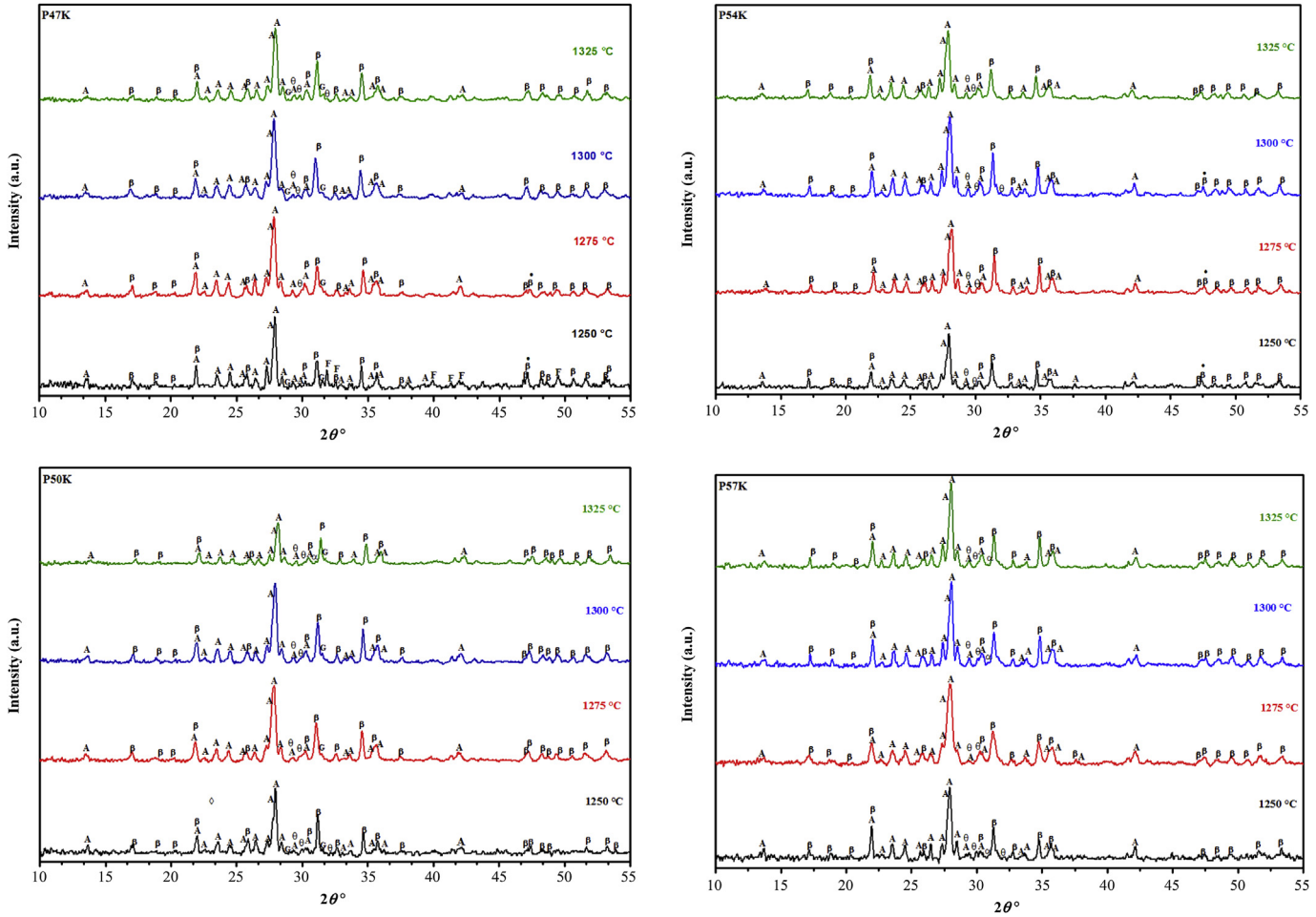

Fig. 7. XRD analysis of each composition sintered at various temperatures revealing the presences of anorthite (A), fluorapatite (F), β-TCP (β), TTCP (θ), gehlenite (G) and fluorite (●).

(gehlinite) which remained in the mixture until 1200 °C. In another research, Kavalci et al. [32] studied the influence of various processing parameters on the development of anorthite ceramics from Sivas kaolin and calcite. They found that the treatment temperature and milling speed were the most significant factors affecting the anorthite crystallization. The authors showed that a milling speed of 200 rpm followed by sintering the compacts at 900 °C for 1 h were sufficient to produce a well-crystallized anorthite phase in the sintered body. Sutcu et al. [14] prepared porous anorthite-based refractory bricks using different clay materials as silica and alumina sources, and paper processing residues as the calcium source. It was found that mixture with low amount of calcium (less than 50%) exhibited the presence of anorthite as the major phase along with mullite as a minor phase. For composition having higher amounts of calcium, gehlinite phase was present in samples sintered at low temperature, below 1350 °C. Similarly, Qin et al. [11] investigated the development of anorthite prepared from lime mud collected from the recycling process of papermaking as the calcium source mixed with fly ash taken from a power plant. The authors found that anorthite was the major phase in all mixtures. Also, the intensity of anorthite peaks was found to increase along with the diminishing of the mullite, gehlinite and quartz from the matrix as the temperature was increase to 1100 °C in accordance to the following reactions:

$$\underset{mullite}{3Al_2O_3.2SiO_2} + 6CaO + \rightarrow \underset{cristobalite}{SiO_2} \rightarrow \underset{gehlinite}{3Ca_2Al_2SiO_7} \quad (5)$$

$$\underset{gehlinite}{3Ca_2Al_2SiO_7} + \underset{mullite}{3Al_2O_3.2SiO_2} + \underset{cristobalite}{7SiO_2} \rightarrow \underset{anorthite}{6CaAl_2Si_2O_8} \quad (6)$$

In agreement with the work of Qin et al., Ptáček et al. [32] who also studied the mixture of kaolin and calcite without intensive milling (2 min) reported the formation of gehlinite along with some wollastonite as an intermediate phase in accordance to Eq. (7). These authors also found that the intermediate phase becomes more prominent when sintered at 1300 °C.

$$\underset{mullite}{3Al_2O_3.2SiO_2} + 7CaO + \underset{cristobalite}{2SiO_2} \rightarrow \underset{gehlinite}{3Ca_2Al_2SiO_7} + \underset{wollastonite}{CaSiO_3} \quad (7)$$

On the contrary, the absence of gehlinite and wollastonite in the present ceramic composites could be associated to a homogeneous mixture attained by wet milling for 5 h at 300 rpm and the initial heat treatment performed on all the powders at 1100 °C prior to sintering which believed to have stabilized the crystalline anorthite phase as evident from the FTIR analysis of the calcined powders as shown in Fig. 6. The results indicated that the peaks at 942 cm^{-1}, 1099 cm^{-1} and a shoulder at 1150 cm^{-1} belongs to the antisymmetric stretching vibration of SiO_4 tetrahedra and Si-O-Al stretching vibration in anorthite phase [21,23,33]. In addition, the bands at 734 cm^{-1} and 757 cm^{-1} could possibly be associated with the feldspar group [21]. The peak at 675 cm^{-1} can be assigned to the vibration of AlO_4 or SiO_4, and at 618 cm^{-1} is due to the stretching of intertetrahedral bonds typical for an ordered crystal structure [34].

On the other hand, the bands at 543 cm^{-1}, 573 cm^{-1} and 606 cm^{-1} correspond to tropical degenerate antisymetric bending υ_4 of PO_4^{3-} group, while the stretching υ_3 of PO_4^{3-} groups results in the bands at 1048 cm^{-1} and 1099 cm^{-1} [21,23]. In addition, υ_2 vibration mode of PO_4^{3-} group appears at 473 cm^{-1} [21]. However, the υ_1 vibration mode

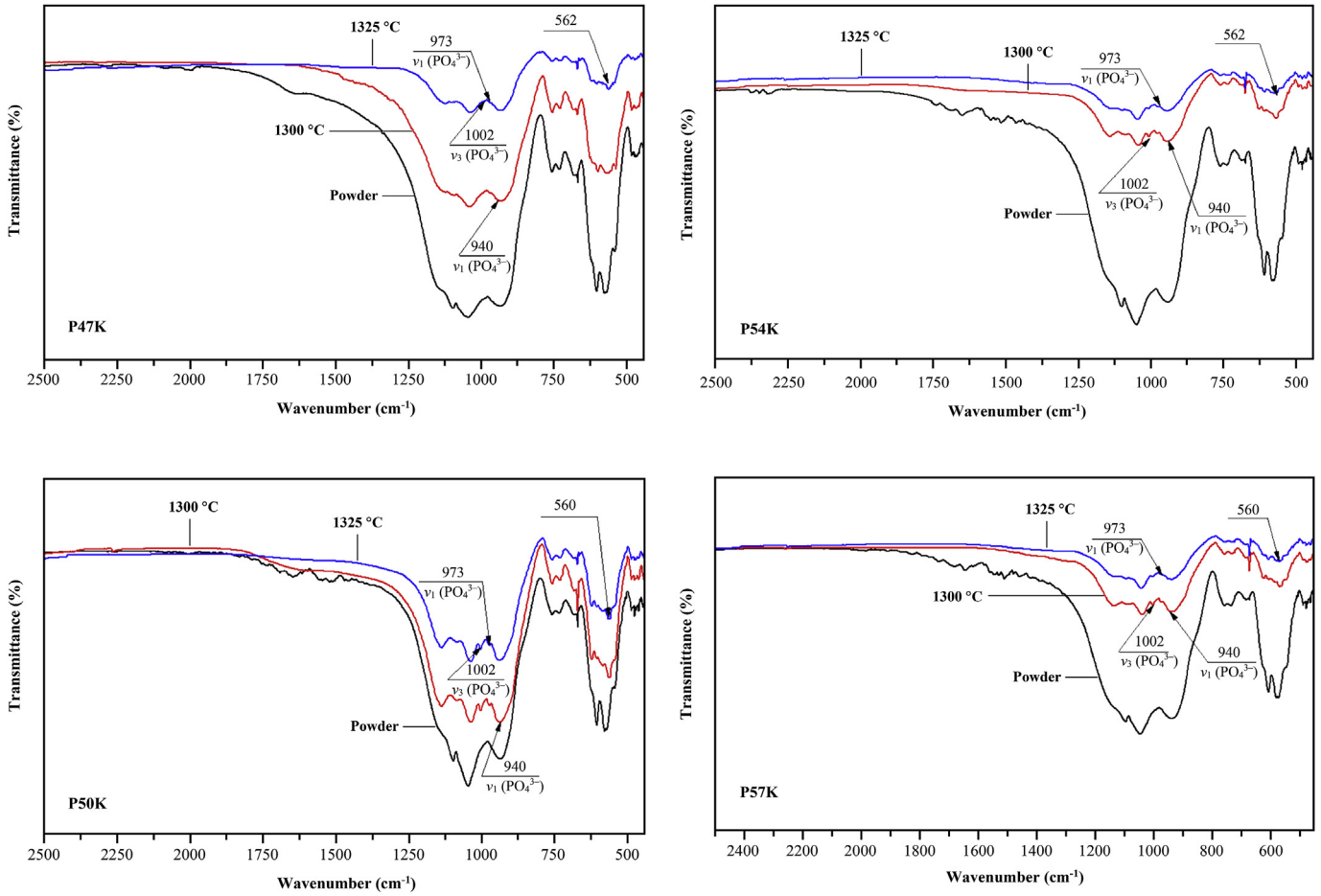

Fig. 8. FTIR spectrum comparison of samples sintered at 1300 °C and 1325 °C for the different mixtures.

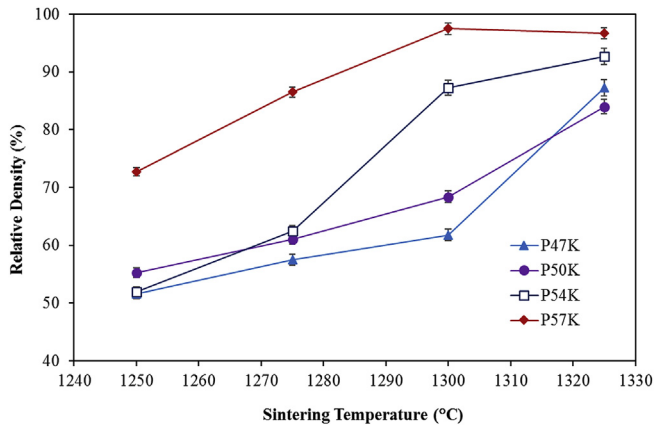

Fig. 9. Relative density variation with sintering temperatures of the sintered samples.

of PO_4^{3-}did not appear due to the overlapping between the bands of anorthite and fluorapatite. Moreover, the characteristic bands for carbonate as observed in Fig. 2 (i.e. 876, 1427 and 1457 cm^{-1}) disappeared after calcination at 1100 °C.

The XRD patterns of the ceramic composites sintered at different temperatures are shown in Fig. 7. The major phases in all the samples have been identified as anorthite and β-TCP (ICDD # 009–0169). In addition, when the sintering temperature increases, the peaks of the anorthite and β-TCP become sharper. The fluorapatite phase as observed in the calcined powders has transformed to β-TCP during sintering. The possible reactions associated with the dissociation of fluorapatite can be expressed as below [35,36]:

$$\underset{fluorapatite}{Ca_{10}(PO_4)_6F_2} + H_2O \rightarrow \underset{\beta-TCP}{2Ca_3(PO_4)_2} + \underset{TTCP}{Ca_4(PO_4)_2O} + 2HF \quad (8)$$

$$\underset{fluorapatite}{Ca_{10}(PO_4)_6F_2} \rightarrow \underset{\beta-TCP}{3Ca_3(PO_4)_2} + \underset{fluorite}{CaF_2} \quad (9)$$

$$\underset{fluorapatite}{3Ca_{10}(PO_4)_6F_2} \rightarrow \underset{\beta-TCP}{2Ca_3(PO_4)_2} + \underset{TTCP}{6Ca_4(PO_4)_2O} + 2POF_3 \quad (10)$$

The FTIR spectrums of these sintered samples which are presented in Fig. 8 shows good correlation with the XRD observation. A new IR bands were noted at 973 cm^{-1} and 940 cm^{-1} corresponding to υ_1 vibration mode of the PO_4^{3-} group of β-TCP, as well as a peak shoulder at about 1002 cm^{-1} which is assigned to υ_3 vibration mode of PO_4^{3-} group in β-TCP structure [37]. In addition to the other bands which appear before sintering, the peak at about 560–562 cm^{-1} signifies the formation of anorthite phase in the ceramic matrix upon sintering [8].

The variation in relative density with sintering temperatures for the sintered samples containing different kaolin content is shown in Fig. 9. In general, it can be seen that the variation in relative density is directly proportional to the kaolin content and the sintering temperature. Both the P47K and P50K compositions exhibited a similar density trend i.e. the relative density increased from 51 to 55% at 1250 °C to 84–87% at 1325 °C. The density of the P54K sample started low as well at about 52% of theoretical density but increased rapidly to reach about 93% when sintered at 1325 °C. In contrast, the sample with the highest kaolin content (P57K) exhibited high relative density when sintered at 1250 °C i.e. about 73% and increased steadily with increasing temperature to attained almost fully dense body (97% of theoretical density) when sintered at 1325 °C.

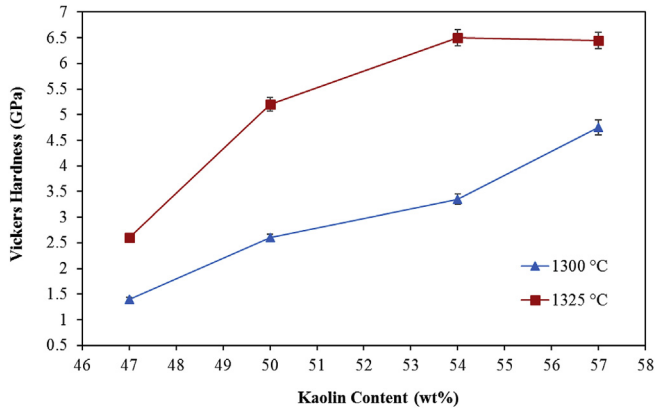

Fig. 10. Variation of Vickers microhardness as a function of kaolin content for samples sintered at 1300 °C and 1325 °C.

This enhance densification, particularly for P57K sample which contained high amount of kaolin, could be associated with the higher amount of liquid phase present during sintering which facilitated particle rearrangement and consolidation. In addition, the presences of mullite, cristobalite (as observed in the calcined powders before sintering) along with the CaO which was made available from the flouroapatite phase dissolution during sintering could have facilitated the formation of a eutectic at about 1170 °C [38]. It can be inferred that as the kaolin content decreases so would the amount of mullite and cristobalite in the calcined powder. This in turn would have an impact in reducing the liquid phase during sintering and hence result in lower densification as observed for the P47K and P50K samples. Another plausible reason could be associated with the phases present in the sintered samples. The results of the semi-quantitative analysis of the different sintered mixtures (Fig. 5) show that the percentage of anorthite that present in the P57K after sintering at different temperatures was higher than for the other samples, and the percentage of β-TCP was lowest in the sintered P57K than for the other samples. It is likely that the higher amount of anorthite present in the matrix is important for promoting a dense structure.

The Vickers microhardness results of the samples sintered at 1300 °C and 1325 °C are shown in Fig. 10. It can be observed that the hardness increases with increase in kaolin content and sintering temperature. As expected, sintering at higher temperatures promoted densification and hardness. The highest hardness of about 6.5 ± 0.7 GPa was attained for samples containing 54 wt% and 57 wt% kaolin sintered at 1325 °C. The hardness variation in this study could be related to two causes; the increase in the percentage of anorthite in the mixtures with the increase

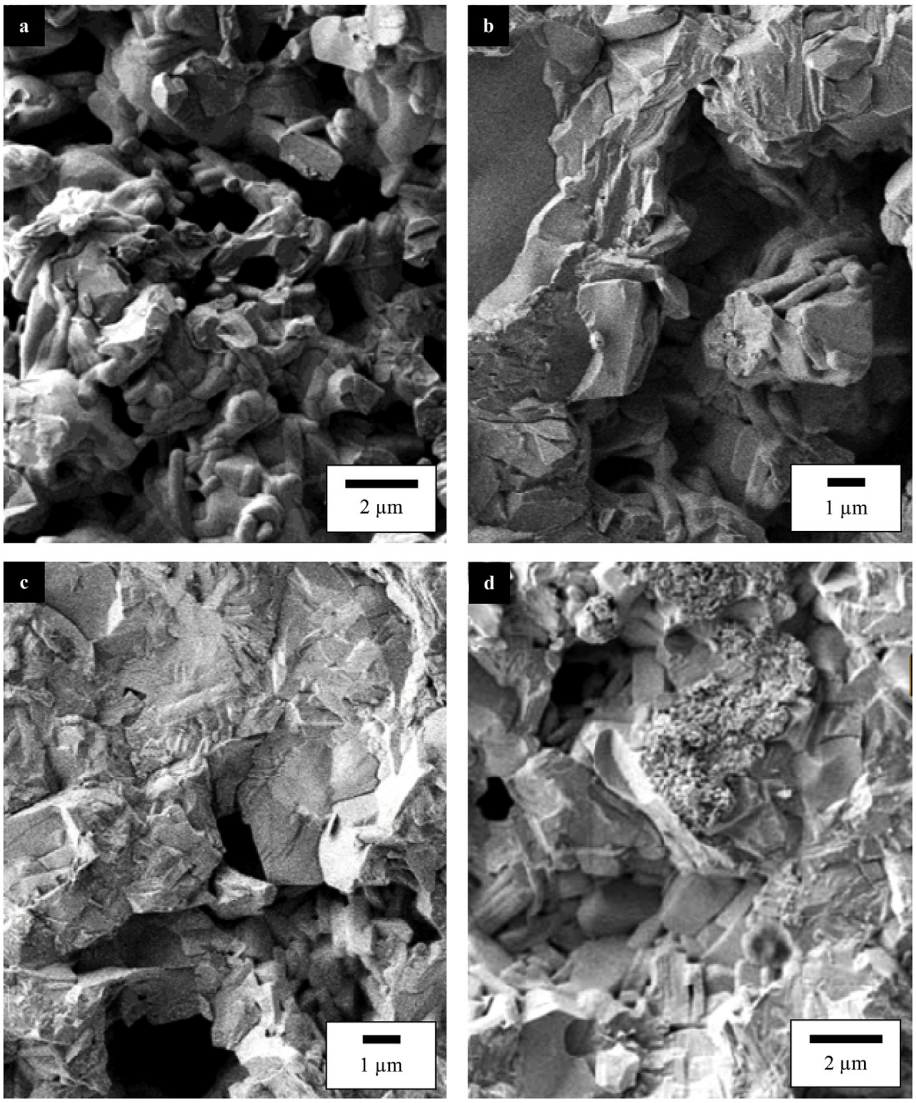

Fig. 11. SEM micrographs of fracture surface for samples sintered at 1325 °C: (a) P47K, (b) P50K, (c) P54K and (d) P57K.

in temperature and the increase in the percentage of kaolin resulting in improvement in densification. This high value of 6.5 ± 0.7 GPa obtained in the present work is in good agreement with the microhardness of an anorthite-fluorapatite based glass-ceramic from a eutectic system [39]. In addition, it has been reported that the hardness of monolithic TCP ceramics when sintered at 1300–1400 °C varied between 2.92 to 3.19 GPa [40]. Thus the obtained hardness for the anorthite-TCP composite in this work is double that of the monolithic TCP and hence would be an added advantage when use as biomaterial.

The microstructural evolution of samples sintered at 1325 °C is shown in Fig. 11. The absences of microcracking in the microstructure shows the feasibility of having a hybrid structure comprising of anorthite intermingled with tricalcium phosphate forming a solid structure despite both having a large difference in the thermal expansion coefficient. It is envisage that the glassy phase present during the formation of anorthite could have accommodated the differential in thermal expansion mismatch between the two components upon cooling to room temperature. More work would be required to elucidate this phenomenon. The microstructure in Fig. 11 also shows that the porosity decreases with the increased in kaolin content in the sintered bodies which supports the high relative density results presented in Fig. 9. Grain coarsening resulting from a liquid phase sintering is also visible with increasing kaolin content. Moreover, close observation of the fracture surfaces indicated the presences of a lamellar structure which extend randomly, believed to be those of anorthite [6,41].

4. Conclusions

In the present work, anorthite-TCP ceramic was prepared for the first time from reacting natural phosphate with kaolin and subjecting the mixture to sintering process in air atmosphere. The study shows that the processing steps adopted was feasible to produce a highly dense composite body. The phase analyses with XRD and supported by FTIR analyses showed that all the mixtures composed of β-TCP intermingle well with anorthite as the major phases without causing any distortion or microcracking. Furthermore, it was found that densification of the samples improved significantly with the increased in the kaolin content and sintering temperatures. Samples from the mixture with low kaolin showed high porosity and high β-TCP content. In contrast, a highly dense body (relative density of 97%) was obtained for samples containing higher anorthite content. A high hardness of 6.5 ± 0.7 GPa was obtained for samples containing 57 wt% kaolin and when sintered at 1300–1325 °C. The results obtained in this study shows that the derived anorthite-TCP has promising characteristics that could be exploited for biomedical application.

References

[1] Y. Kobayashi, E. Kato, Low- temperature fabrication of anorthite ceramics, J. Am. Ceram. Soc. 77 (1994) 833–834.
[2] R. Ceylantekin, Production of mono-anorthite phase through mechanical activation, Ceram. Int. 41 (2015) 353–361.
[3] Y. Han, C. Li, C. Bian, S. Li, C.-A. Wang, Porous anorthite ceramics with ultra-low thermal conductivity, J. Eur. Ceram. Soc. 33 (2013) 2573–2578.
[4] C. Li, Y. Han, L. Wu, K. Chen, L. An, Fabrication and properties of porous anorthite ceramics with modelling pore structure, Mater. Lett. 190 (2017) 95–98.
[5] Y. Li, X. Cheng, L. Gong, J. Feng, W. Cao, R. Zhang, H. Zhang, Fabrication and characterization of anorthite foam ceramics having low thermal conductivity, J. Eur. Ceram. Soc. 35 (2015) 267–275.
[6] X. Cheng, S. Ke, Q. Wang, H. Wang, A. Shui, P. Liu, Fabrication and characterization of anorthite-based ceramic using mineral raw materials, Ceram. Int. 38 (2012) 3227–3235.
[7] S. Zaiou, A. Harabi, E. Harabi, A. Guechi, N. Karboua, M.-T. Benhassine, S. Zouai, F. Guerfa, Sintering of anorthite based ceramics prepared from kaolin DDR and calcite, Ceramica 62 (2016) 317–322.
[8] I. Perná, M. Šupová, T. Hanzlíček, Gehlenite and anorthite formation from fluid fly ash, J. Mol. Struct. 1157 (2018) 476–481.
[9] H. Hu, L. Dai, H. Li, K. Hui, J. Li, Temperature and pressure dependence of electrical conductivity in synthetic anorthite, Solid State Ionics 276 (2015) 136–141.
[10] N.T. Selli, Development of anorthite based white porcelain stoneware tile compositions, Ceram. Int. 41 (2015) 7790–7795.
[11] J. Qin, C. Cui, X. Cui, A. Hussain, S. Yang, Recycling of lime mud and fly ash for fabrication of anorthite ceramic at low sintering temperature, Ceram. Int. 41 (2015) 5648–5655.
[12] C.-W. Wu, C.-J. Sun, S.-H. Gau, C.-L. Hong, C.-G. Chen, Mechanochemically induced synthesis of anorthite in MSWI fly ash with kaolin, J. Hazard Mater. 244–245 (2013) 412–420.
[13] S. Kurama, E. Ozel, The influence of different CaO source in the production of anorthite ceramics, Ceram. Int. 35 (2009) 827–830.
[14] M. Sutsu, A. Akkurt, Utilization of recycled paper processing residues and clay of different sources for the production of porous anorthite ceramics, J. Eur. Ceram. Soc. 30 (2010) 1785–1793.
[15] M. Sutcu, S. Akkurt, A. Bayram, U. Uluca, Production of anorthite refractory insulating firebrick from mixtures of clay and recycled paper waste with sawdust addition, Ceram. Int. 38 (2012) 1033–1041.
[16] S.M. Naga, M. Sayed, H.F. Elmaghraby, M. Sh Khalil, M.A. EL-Sayed, Fabrication and properties of cordierite/anorthite composites, Ceram. Int. 43 (2017) 6024–6028.
[17] C. Li, C. Bian, Y. Han, C. Wang, L. An, Mullite whisker reinforced porous anorthite ceramics with low thermal conductivity and high strength, J. Eur. Ceram. Soc. 36 (2016) 761–765.
[18] Z. Miao, N. Li, W. Yan, Effect of sintering temperature on the phase composition and microstructure of anorthite–mullite–corundum porous ceramics, Ceram. Int. 40 (2014) 15795–15799.
[19] K. Hua, A. Shui, L. Xu, K. Zhao, X. Xi, Fabrication and characterization of anorthite–mullite–corundum porous ceramics from construction waste, Ceram. Int. 42 (2016) 6080–6087.
[20] J. Liu, Y. Dong, X. Dong, S. Hampshire, L. Zhu, Z. Zhu, L. Li, Feasible recycling of industrial waste coal fly ash for preparation of anorthite-cordierite based porous ceramic membrane supports with addition of dolomite, J. Eur. Ceram. Soc. 36 (2016) 1059–1071.
[21] S. Agathopoulos, D.U. Tulyaganov, P.A.A.P. Marques, M.C. Ferro, M.H.V. Fernandes, R.N. Correia, The fluorapatite–anorthite system in biomedicine, Biomaterials 24 (2003) 1317–1331.
[22] H. Belhouchet, F. Chouia, M. Hamidouche, A. Leriche, Preparation and characterization of anorthite and hydroxyapatite from Algerian kaolin and natural phosphate, J. Therm. Anal. Calorim. 126 (2016) 1045–1057.
[23] B. Samuneva, Y. Ivanova, P. Djambaski, S. Stefanova, Y. Dimitriev, M. Dimitrova-Lukacs, Phase formation in gels of the apatite-anorthite system, J. Sol. Gel Sci. Technol. 13 (1998) 255–259.
[24] M.U. Taskiran, N. Demirkol, A. Capoglu, A new porcelainised stoneware material based on anorthite, J. Eur. Ceram. Soc. 25 (2005) 293–300.
[25] M. Pal, S. Das, S.K. Das, Anorthite porcelain: synthesis, phase and microstructural evolution, Bull. Mater. Sci. 38 (2015) 551–555.
[26] M.B. Sedel'nikova, V.M. Pogrebenkov, Production of ceramic pigments with diopside and anorthite structure using the gel method, Glass Ceram. 63 (2006) 271–273.
[27] A. Tunali, E. Ozel, S. Turan, Production and characterisation of granulated frit to achieve anorthite based glass–ceramic glaze, J. Eur. Ceram. Soc. 35 (2015) 1089–1095.
[28] A. Antonakos, E. Liarokapis, T. Leventouri, Micro-Raman and FTIR studies of synthetic and natural apatites, Biomaterials 28 (2007) 3043–3054.
[29] J. Perrone, B. Fourest, E. Giffaut, Surface characterization of synthetic and mineral carbonate fluoroapatites, J. Colloid Interface Sci. 249 (2002) 441–452.
[30] T. Sahraoui, H. Belhouchet, M. Heraiz, N. Brihi, A. Guermat, The effects of mechanical activation on the sintering of mullite produced from kaolin and aluminum powder, Ceram. Int. 42 (2016) 12185–12193.
[31] M. Mouiya, A. Abourriche, A. Bouazizi, A. Benhammou, Y. El Hafiane, Y. Abouliatim, L. Nibou, M. Oumam, M. Ouammou, A. Smith, H. Hannache, Flat ceramic microfiltration membrane based on natural clay and Moroccan phosphate for desalination and industrial wastewater treatment, Desalination 427 (2018) 42–50.
[32] S. Kavalci, E. Yalamaç, S. Akkurt, Effects of boron addition and intensive grinding on synthesis of anorthite ceramics, Ceram. Int. 34 (2008) 1629–1635.
[33] G. Yilmaz, Structural characterization of glass–ceramics made from fly ash containing SiO_2–Al_2O_3–Fe_2O_3–CaO and analysis by FT-IR–XRD–SEM methods, J. Mol. Struct. 1019 (2012) 37–42.
[34] P. Castaldi, L. Santona, C. Cozza, V. Giuliano, C. Abbruzzese, V. Nastro, P. Melis, Thermal and spectroscopic studies of zeolites exchanged with metal cations, J. Mol. Struct. 734 (2005) 99–105.
[35] N. Bouslama, F. Ben Ayed, J. Bouaziz, Sintering and mechanical properties of tricalcium phosphate–fluorapatite composites, Ceram. Int. 35 (2009) 1909–1917.
[36] K. Tonsuaadu, K.A. Gross, L. Plūduma, M. Veiderma, A review on the thermal stability of calcium apatites, J. Therm. Anal. Calorim. 110 (2011) 647–659.
[37] B.O. Fowler, E.C. Moreno, W.E. Brown, Infra-red spectra of hydroxyapatite, octacalcium phosphate and pyrolysed octacalcium phosphate, Arch. Oral Biol. 11 (1966) 477–492.
[38] S. Nath, K. Biswas, K. Wang, R.K. Bordia, B. Basu, Sintering, phase stability, and properties of calcium phosphate-mullite composites, J. Am. Ceram. Soc. 93 (2010) 1639–1649.
[39] H.A. Abo-Mosallam, E.A. Mahdy, H.C. Park, Crystallisation characteristics and properties of glasses based on fluorapatite–anorthite eutectic system, Mater. Res. Innov. 17 (2013) 167–171.
[40] C.X. Wang, X. Zhou, M. Wang, Influence of sintering temperature on hardness and Young's modulus of tricalcium phosphate bioceramic by nanoindentation technique, Mater. Char. 52 (2004) 301–307.
[41] A. Dimanov, G. Dresen, X. Xiao, R. Wirth, Grain boundary diffusion creep of synthetic anorthite aggregates: the effect of water, J. Geophys. Res. 104 (1999) 10483–10497.